Catalysis Science & Technology

Accepted Manuscript

ROYAL SOCIETY OF CHEMISTRY

www.rsc.org/catalysis

Photocatalytic hydrogen evolution from cobalt/nickel complex with dithiolene ligand under the irradiation of visible light

Heng Rao[1, †], Zhi-Yuan Wang[1, †], Hui-Qin Zheng[1, 2], Xiao-Bo Wang[1],

Chun-Mei Pan[3], Yao-Ting Fan [1,*], Hong-Wei Hou[1]

1. College of Chemistry and Molecular Engineering, Zhengzhou University, Zhengzhou 450001, PR China

2. Department of Chemistry, Henan Institute of Education, Zhengzhou 450046, PR China

3. Biotechnology Department, Henan University of Animal Husbandry and Economy, Zhengzhou 450011, PR China

Abstract： Two novel metal dithiolene complexes, namely $N^tBu_4[M(BNT)_2]$ [M=Co/Ni, (BNT=(R)-1, 1'-Binaphthalene-2, 2'-dithiol)], had been synthesized and characterized. An efficient homogeneous photocatalytic system was constructed by combination of the noble-metal-free target complexes as water reduction catalyst, xanthene dyes as photosensitizer and triethylamine (TEA) as the sacrificial electron donor under the irradiation of visible light (λ>420 nm). The maximum H_2 evolution of 495/676 turnovers (vs. Catalyst) was recorded under the optimal conditions in CH_3CN/H_2O (1:1, v/v) after 4 h of irradiation. Furthermore, the mechanism of H_2 evolution was also briefly discussed by fluorescence spectrum and cyclic voltammetry studies.

Key words: Cobalt/nickel dithiolene complex; Synthesis; Photocatalysis; Hydrogen evolution; Mechanism.

* Corresponding author. Tel/fax: +86 (0) 371- 67766017.

E-mail addresses: yt.fan@zzu.edu.cn /ytfan1207@163.com

†These authors contributed equally.

1. Introduction

Molecular hydrogen is one of the most promising and cleanest energy carriers in the future because of its least negative effect on the environment.[1, 2] Photocatalytic H_2 evolution utilizing solar energy is energy-efficient and zero emission, providing a new alternative to environmental and energy issues as well as a platform for the hydrogen economy.[3] Therefore it has attracted considerable attention on account of its high calorific value and producing only water upon combustion as well as potential applications in clean energy production, recycling utilization of renewable resource, reducing the consumption of fossil fuel and environmental protection.[4] A typical photocatalytic water reduction system usually contains three components: a water-reducing catalyst (WRC), a light-absorbing photosensitizer (PS) and a sacrificial reductant (SR) which replaces the complex water oxidation half-reaction. In the past few years, a mountain of work done in this area involves the use of noble-metal-based PSs or WRCs.[5-8] Obviously, developing a photocatalytic system with noble-metals-free PS and WRC is an alluring topic to improve the hydrogen production efficiency and stability of photocatalytic system.

As we all know, the complex $Co(bpy)_3^{2+}$ and other polypyridyl cobalt complexes have been used as "first generation" noble-metal-free catalysts for H_2 generation.[9-15] Although a number of them were good initial catalysts, their activity was greatly limited in photocatalytic H_2 evolution by visible light-driven. Until recently, only a few noble-metals-free photocatalysts had been prepared for photoreduction of water to generate hydrogen under visible light.[16-18] For instance, the DuBois' series of nickel(II) molecule catalysts with amine base-containing diphosphine ligands are very impressive cases.[19-22] One of them was utilized as a catalyst for photocatalytic hydrogen generation from water, and the maximum TONs of 2700 over 150 h was observed with $Ru(bpy)_3^{2+}$ (bpy=bipyridine) as photosensitiser (PS) and ascorbic acid as sacrificial agent.[18] In addition, several types of cobalt thiolates[23, 24] and nikel thiolates[25-27] were also successively synthesized for photogeneration of hydrogen. For example, a high hydrogen evolution of 2700 TONs in 16 h was obtained from the complex $[Co(BDT)_2]^-$ (BDT = 1,2-benzenedithiolate) with $Ru(bpy)_3^{2+}$ as PS and ascorbic acid as the sacrificial electron donor as described by Eisenberg and co-workers. After that, a maximum hydrogen evolution of 9000 TONs was also reported from the complex $(TBA)[Co(MNT)_2]$ (MNT = maleonitriledithiolate) in 20 h under similar conditions by the same study group. However, the noble-metal-based PS, namely $Ru(bpy)_3^{2+}$, was still used in these

photocatalytic systems. To overcome this issue, Beller et al. developed a noble-metal-free sensitizer based on a copper(I) complex with polypyridine ligands, affording about 480 TONs (vs. PS) of H_2 in combination with $Fe_3(CO)_{12}$ in a mixture of THF, water, and triethylamine (4:1:1, v/v/v) in 24 h irradiation with visible light.[28] More recently, xanthene dyes as high efficient PSs were already used in homogeneous hydrogen production systems.[29, 30] In the present work, EY^{2-} was chosen as the PS in which the heavy atoms could facilitate the formation of a long-lived triplet state, resulting in the efficient transfer of electrons to the catalyst. And EY^{2-} always displayed much higher hydrogen production activity in the literatures.[29, 31]

So far, the efforts to design and investigate a new photocatalytic system solely based on noble-metal-free catalyst are still considerably lacking for photoreduction of water to generate hydrogen under the irradiation of visible light. Especially, it is challenging scientific community in the field to develop effective, long-life and inexpensive new-type noble-metals-free catalysts. Thus more efforts should be made for the above purpose.

Nickle is a metal active center in [FeNi]-Hases (Hases=hydrogenase) which plays a critical role in releasing hydrogen in the natural world. Additionally, the mimics of vitamin B_{12}, namely cobaloxime and its derivatives, were also used as photocatalyst and displayed a relative high H_2 generation activity in some photocatalytic systems.[31, 33] On the other hand, metal thiolates are also an attractive class of compounds which have been investigated since the 1960s [34] and draw our attention because of their unique structures which can be modified by substituents. In the present paper, we attempted to design new photocatalyst based on cobalt/nickel dithiolene complex, in which the compound BNT containing S donors was employed as bidentate ligand based on its electron-poor property and structure characteristics with both rigid and tenacious group (BNT presents (R)-1, 1'-binaphthalene-2, 2'-dithiol, see Scheme 1). Thus, the structure of the title complexes, such as the electronic environment around the metal ion centre, could be modified by adjusting the rigid or flexible group in the ligand. When the bidentate thiolates bear such an aromatic moiety, the electron density can substantially be diverted away from the monometallic center upon reduction. And as a result of the conjugating effect of the aromatic system which can buffer the electron density of the metal center, the reducibility of the catalysts can be significantly improved by lowering their potentials.

In light of the above considerations, two novel bio-inspired complexes, namely $N^tBu_4[M(BNT)_2]$

[M=Co/Ni (**1/2**)], had been synthesized and characterized. And then the H_2 evolution performance of the target samples was further evaluated using the constructed noble-metal-free photocatalytic system under the irradiation of visible light. In addition, the mechanism of hydrogen evolution was also briefly discussed by fluorescence spectra and cyclic voltammetry measurements.

Scheme 1

2. Experimental section

2.1 Reagents and instruments

All reagents were of analytical purity, purchased through traditional commercial channels and used without further purification. All reactions and operations were carried out under dry nitrogen atmosphere with standard Schlenk techniques. All solvents were dried and distilled prior to use according to the standard methods.[35] IR spectra were recorded on a Nicolet IR 470 spectrophotometer. EPR spectra was measured on a JES FA200 instrument at T =298 K, ν =9.065 GHz, P_{mw}= 0.998 mW and modulation amplitude 0.1 mT. ^{1}H NMR spectra were recorded on a Bruker DRX (400 MHz) instrument. Elemental analyses were performed on a Carlo-Erba 1160 elemental analyzer. UV-vis absorption spectra were recorded using a Hitachi U-2000 spectrophotometer (200-1100 nm) and the absorption measurement was achieved in a 1 cm quartz cell. The pH was determined by a PHS-25 pH meter. The fluorescence spectra were recorded in CH_3CN/H_2O (1: 1, v/v) with a HITACHI F-4500 fluorescence spectrophotometer. Cyclic voltammetry (CV) experiments were conducted on a CHI630B electrochemical workstation equipped with a glassy carbon working electrode, a Pt auxiliary electrode, and a SCE(standard calomel electrode) as reference electrode, and the CV measurement was achieved in 0.1 M n-Bu_4NPF_6 of CH_3CN or KNO_3 of 1: 1 CH_3CN/H_2O (v/v).

2.2 Preparation of $N^tBu_4[Co(BNT)_2]$ (1)

(R)-1, 1'-Binaphthalene-2, 2'-dithiol was prepared from known procedures using (R)-1, 1'-binaphthol as the precursor and the spectral data were well agreed with that reported in the literature.[36] In a 100 mL Schlenk vessel, $Co(BF_4)_2{\cdot}6H_2O$ (276 mg, 0.81 mmol) and KO^tBu (333 mg, 3.0 mmol) were dissolved in 30 mL of dry MeOH in the N_2 atmosphere and allowed to stir at room temperature for 1h. And then, a degassed mixture of BNT (509 mg, 1.67 mmol) in MeOH (10 mL)

was added dropwise into the above solution. The mixture was continually stirred for 4 h at room temperature when its color darkened to deep blue. A solution of N^tBu_4Br (396 mg, 1.23mmol) in 5 mL MeOH was added dropwise into the above reaction mixture. Thereafter the N_2 atmosphere was removed from Schlenk vessel, and the mixed solution was allowed to stir at room temperature overnight. Vacuum evaporation to remove most of the solvent (reservations about 10 mL), a dark blue precipitate was obtained. The synthetic route of **1** was listed in Scheme 2. The crude solid was collected and recrystallized from a mixture of dichloromethane and ether to yield **1** as a blue crystalline solid (312 mg, 0.51 mmol, 59% yield). IR (KBr pellet): ν =3424, 3046, 2951, 2870, 1664, 1614, 1579, 1499, 1383, 1310, 1255, 1124, 942, 808, 772, 742, 666 cm^{-1}. ^1H NMR (400 MHz, $CDCl_3$) δ=7.96(dd, 8H), 7.56(d, 4H), 7.40(m, 4H), 7.25(m, 4H), 7.01(d, 4H), 3.10(m, 8H), 1.60(q, 8H), 1.38(q, 8H), 0.98(t, 12H) ppm. Anal. Calcd (%) for $C_{56}H_{60}NCoS_4$: C, 77.99; H, 6.47; N, 1.50; Found: C, 77.91; H, 6.46; N, 1.50. ESI MS: m/z 933.29 (expected), 933.01 (found).

Scheme 2

*2.3 Preparation of $N^tBu_4[Ni(BNT)_2]$ (**2**)*

Preparative method of *$NBu_4[Ni(BNT)_2]$ (**2**)* was the same as that of **1**, except that $Co(BF_4)_2{\cdot}6H_2O$ was replaced by $Ni(BF_4)_2{\cdot}6H_2O$. The following operation was handled as stated in Section 2.2 to give a blue black solid (338mg, 0.55 mmol, 64% yield). EPR spectra of $Ni(BNT)_2^-$ was measured on JES FA200, experimental conditions: T =298 K, ν =9.065 GHz, P_{mw}= 0.998 mW, modulation amplitude 0.1 mT.(See Fig. 2S) The **g** matrix determined from the observed EPR spectra of paramagnetic nickel complexes was **g** = [2.043, 2.017, 1.998]. The values were characteristic of the low-spin $3d^7$ electronic configuration, which proved to be a three-valence Ni(III) complex.[37] IR (KBr pellet): ν =3425, 3045, 2956, 2870, 1665, 1614, 1580, 1500, 1420, 1384, 1346, 1254, 1121, 1054, 943, 809, 772, 742, 694 cm^{-1}. Anal. Calcd (%) for $C_{56}H_{60}NNiS_4$: C, 72.01; H, 6.47; N, 1.50; Found: C, 71.94; H, 6.46; N, 1.50. ESI MS: m/z 932.30 (expected), 932.05 (found).

2.4 Experimental design and procedure for photocatalytic H_2 generation

Photolysis experiments were performed in a homogeneous three-component photocatalytic

system with 40 mL Quartz Glass bottles as the batch reactors with a working volume of 20 mL containing the target complex (**1** / **2**) as the WRC, EY^{2-} as the PS and TEA as the SR in CH_3CN/H_2O (1: 1,v/v) (Scheme 1). The mixture was magnetically stirred under N_2 atmosphere for 10 min to remove all the air and keep the anaerobic environment. The pH value of the medium was adjusted using dilute HCl. Then the solution was irradiated from outside of the bottle using a 300 W Xe lamp with a 420 nm cut-off filter at 25 °C.

The H_2 evolution was measured using Gas Chromatograph (GC, Agilent 4890D) equipped with a thermal conductivity detector (TCD) and a porapak Q stainless column. The temperatures of the injection port, the oven and the detector were 100 °C, 80 °C and 150 °C, respectively. N_2 served as the carrier gas at a flow rate of 20 $mL \cdot min^{-1}$. The total gas volume was measured by releasing the pressure in the bottles using displacement of saturated brine equipment. All the experiments were carried out independently in triplicate.

3. Results and discussion

A three-component homogeneous photocatalytic system was consisted of the target complex (**1/2**) as catalyst, EY^{2-} as PS, and TEA as the SR in CH_3CN/H_2O solution without extra proton source under the irradiation of visible light (λ>420nm). The key parameters that affected the evolution of H_2 were optimized in the photocatalytic process.

3.1 Effect of solvent on hydrogen generation

Both the solvent kinds and the ratio of organic solvent to water (v/v) notably affected H_2 generation in the photocatalytic system. Fig. 1 depicted the effect of solvent kinds on H_2 generation at the fixed conditions with **1** of 0.1 mM, EY^{2-} of 0.4 mM and 10% TEA (v/v) at pH 10.0 under irradiation of visible light (λ>420 nm). As shown in Fig. 1, the H_2 generation was significantly affected by solvent kinds in the photocatalytic process. The maximum TONs (495) appeared in the mixed solvent of CH_3CN/H_2O (v/v 1:1) after 4 h irradiation. When the volume ratio of CH_3CN/H_2O deviated from 1:1, the hydrogen evolution was dramatically decreased. For instance, the hydrogen evolution of 202 TONs and 282 TONs was recorded when the volume ratios of CH_3CN/H_2O were 1:4 and 4:1, respectively. The results indicated that the volume ratio of CH_3CN/H_2O significantly affected the H_2 evolution in the photocatalytic system because the properties of solvent, such as polarity, dielectric constant and diffusion coefficient, significantly affected photocatalytic reaction.[30]

Fig. 1

Interestingly, a small quantity of H_2 (8.0 TON, vs. catalyst) was found in the pure water with 4 h irradiation, implying that water was also an essential factor to affect the H_2 generation in the photocatalytic reaction. The reason should be very intricate, and we speculated that one of them was that those photocatalysts only existed in the form of suspended matter and were slightly soluble in pure water (heterogeneous solution), resulting in more difficult photoinduced electron transfer from the PS to the photocatalyst. In this case, the active intermediate species could not be formed or were difficult to be formed, inhibiting H_2 production activity of photocatalysts. However, water was an indispensable component in the photocatalytic system. The speculation had been proved in a similar photocatalytic system composed of a cobalt bipyridine complex as the catalyst, $Ru(bpy)_3^{2+}$ as the PS, ascorbate as the SR and D_2O in place of H_2O as the solvent,[38] in which more than 90% of D_2 had been detected in the gas phase under optimal conditions, indicating that the generated H_2 derived from protons in the water.

3.2 Effect of medium pH on hydrogen generation

To the best of our knowledge, the pH value significantly affects the interaction of PS and catalyst, the state of PS and TEA, and the subsequent driving force for photocatalytic H_2 evolution in the photocatalytic system.[29, 39-40] Fig.2 illustrated the variable trend of H_2 evolution with initial pH value in the range of 7 to 12.

Fig. 2

As shown in Fig. 2, when the pH value of the system was varied from 7 to 12, the maximal TONs of 495 for **1** and 676 for **2** appeared at pH 10, respectively. When the pH value of medium was less than 8.0 or greater than 11.0, the H_2 evolution decreased dramatically. For instance, the H_2 evolution of 64 TONs at pH 7.0 and 89 TONs at pH 12 was only observed for **1**, respectively. No matter what the pH value was, the H_2 evolution activity of **2** was always higher than that of **1** in all cases. The probable reason was due to the difference of redox ability between the two catalysts, which would be further discussed in the electrochemical property section (See section 3.6). The great decrease of TONs at lower pH value was probably because of the protonation of TEA, which

resulted in poor electron-donating ability. On the other hand, in an excessively alkaline medium, the driving force for H_2 evolution would be decreased at a lower concentration of H^+. Additionally, EY^{2-} enabled stronger light absorption at a higher pH value.[41] All of these reasons indicated that the proper pH value of the medium could promote H_2 evolution by the target catalyst, meanwhile, the activity of the catalyst would be inhibited by lower or higher pH values in the photocatalytic process.

*3.3 Effects of molar ratio of PS/catalyst (**1**) on hydrogen generation*

The molar ratio of PS/catalyst is also an important influence factor for hydrogen evolution. Herein, **1** was selected as catalyst to investigate the effect of different molar ratio of PS (EY^{2-}) to catalyst (**1**) on hydrogen evolution, and the result was listed in Table1.

Table 1

As shown in Table 1, the maximum H_2 evolution of 495 TONs appeared at molar ratio of EY^{2-} to **1** of 1:0.25. When the molar ratio of EY^{2-} to **1** was deviated from the value, the H_2 evolution decreased dramatically. For instance, when the molar ratio of EY^{2-} to **1** was changed from 1:0.5 to 1:1 and 4:1, the corresponding hydrogen evolution was reduced from 326 TONs to 152 TONs and 237 TONs, respectively, illustrating that the molar ratio of PS to catalyst considerably impacted hydrogen generation in the system. However, the higher concentration of PS would be unfavourable for diffusion and absorption of visible light in the photolytic system, resulting in the decrease of hydrogen evolution. As stated above, although the molar ratios of PS/ WRC such as "1: 0.25 and 4: 1" or "1: 0.5 and 2: 1" were the same in form, the higher concentration of them led inevitably to a depression of hydrogen evolution. Therefore, the reasonable control for molar quantities ratio of PS to photocatalyst was also an effective strategy to improve the H_2 generation in the photolysis process.

The result suggested that intramolecular electron transition of EY^{2-} from the ground state to the excited state played a crucial role in the photocatalytic process, which led to the molecule structure transformation of dye from enol form to ketone form under the irradiation of visible light. In this case, the excited electron was transmitted to photocatalyst, and then got back to the ground state.

After that, the dye molecule with ketone form structure further got electron from electronic sacrificial agent and got back to the enol form structure, achieving the recycle use of dye.[30]

3.4 Stability of the photocatalytic system

We also found out that the H_2 generation stopped after 4 h irradiation. In order to clarify the reason of deactivity in the photocatalytic system, the following experiments were further arranged.

Fig. 3

Considering TEA was in large excess in the photocatalytic system, the inactivation of system was probably related to photodegradation of PS or catalyst. Thus, the extra EY^{2-} (0.4 mM, 8 μmol) or **1**(0.1 mM, 2 μmol) was added to the photocatalytic system separately after H_2 generation ceased. The result was illustrated in Fig. 3. Only 59 TONs (added **1**) and about 406 TONs (added EY^{2-}) was observed in the next 4 h irradiation as expected. That was to say, the H_2 production activity of the system was restored to about 80% and 12% when extra PS and catalyst **1** were added to the inactive system again, respectively. The experimental verification indicated that the deactivation of photocatalytic system was mainly attributed to the photodegradation of EY^{2-}, and secondly, the complex **1** also had a slight effect on the deactivation of the photocatalytic system.

The speculation was further confirmed by the change of UV/vis absorption spectra of EY^{2-} before and after irradiation with visible light (Fig.3 (b)). As shown in Fig.3 (b), the strong absorption of EY^{2-} at 520nm before irradiation was weakened dramatically and blue-shifted to 496 nm after irradiation of 4 h. Meanwhile, the strength of the absorption peak lessened dramatically with the increase of irradiation time. After undergoing irradiation of 4 h, only a very weak shoulder at 496 nm could be observed, indicating that the EY^{2-} dye was almost completely degraded in the photocatalytic process. The main degradation product was confirmed to be fluorescein compound as reported by literature.[42]

3.5 Kinetics of electron transfer processes in the photocatalytic system

In order to better understand the mechanism of photocatalytic system, the interaction between EY^{2-} and catalyst (**1**/**2**) was investigated by fluorescence measurements. The changes of fluorescence spectra of EY^{2-} (1.0×10^{-5} M) with different catalyst concentrations from 0 to 0.75 mM

for **1** and from 0 to 0.30 mM for **2** in CH_3CN/H_2O (1: 1, v/v) were illustrated in Fig. 4. As shown in Fig. 4, the EY^{2-}gave a strong emission band as expected in the range of 525-600 nm with a maximum peak at 544 nm upon excitation at 527 nm in CH_3CN/H_2O(1:1, v/v) at room temperature. The fluorescence intensity of EY^{2-} was quenched gradually when increasing the concentration of **1** or **2** in EY^{2-} solution. The fluorescence intensity was quenched up to ca. 53% at 544 nm upon addition of 70 equiv of **1**, and ca. 55% at 544 nm upon addition of 30 equiv of **2.** The result indicated that there was a stronger interaction between EY^{2-} and **2** than that between EY^{2-} and **1**, which might resulted in higher hydrogen evolution for **2** than that for **1**. On the basis of the Stern-Volmer plot (the inset in Fig.4), the quenching constant k_q calculated by the equation of $I_0/I = 1+ K_{sv}[Q] = 1+ k_q\tau_0[Q]$ was 2.5×10^{12} $M^{-1}s^{-1}$ for **1** and 5.7×10^{12} $M^{-1}s^{-1}$ for **2**. The present experiment result was also in well agreement with the literature data (8.5×10^{12} $M^{-1}s^{-1}$) as reported by Dong et al., of which RB^{2-} as PS was quenched by $[Co(bpy)_3]Cl_2$ as WRC under the similar conditions.[43] The results suggested that the intermolecular quenching was diffusion-controlled and the direct electron transfer (ET) from singlet excited state ($^{1*}EY^{2-}$) to the catalyst might occur in the photoinduced H_2 evolution system. It was found that the fluorescence quenching of EY^{2-} in CH_3CN/H_2O of 1:1 (v/v) was not observed when an excess of TEA (about 1000 equiv) was added to the photocatalytic system, indicating that the ET did not take place by $^{1*}EY^{2-}$. However, a very slight quenching was also observed in the present system when the overwhelmed dosage of TEA (about ten thousand equiv) was added to the system. The result indicated that most of the excited PS (in the triplet form) was quenched by WRC, and only a small part was quenched by TEA. Because the reductive ET preferentially occurred at long-lived triplet-state species ($^{3*}EY^{2-}$) in this case, which was formed by intersystem crossing (ISC) as reported by previous literature.[44] That was to say, both the species of active $^{1*}EY^{2-}$ and $^{3*}EY^{2-}$ could transported an electon to the photocatalyst.

Fig. 4

*3.6 Electrochemical behavior of **1** and **2***

As the electrochemical behavior of the catalyst significantly affected the ET process and H_2 evolution activity in the photocatalytic system, the electrochemical experiments were arranged to elucidate the mechanism of hydrogen evolution in the present system. So far, most of the well studied electrocatalysts operated in nonaqueous media, whereas efforts on the reductive side of

water splitting would ideally incorporate proton reduction electrocatalysts that operated in largely aqueous environments.[45, 46] Fig.5(a) shows the cyclic voltammograms (CV) of **1** in CH_3CN/H_2O (1:1, v/v) solution containing 0.1 M KNO_3. In the absence of acid, a reversible redox couple was observed at -0.72 V (vs. standard calomel electrode, SCE), that could be attributed to the $Co(BNT)_2^-/Co(BNT)_2^{2-}$ couple. With the addition of trifluoroacetic acid (TFA), the catalytic wave was observed at a more negative potential than the $Co(BNT)_2^-/Co(BNT)_2^{2-}$ reduction, implying that following the initial reduction and protonation, a second, turnover-limiting reduction and protonation occurred to form H_2. In order to show clearly the redox properties of **1** and **2** without acid, we conducted the CV experiment in 0.1 M n-Bu_4NPF_6/CH_3CN.(See Fig.1S) While the metal oxidation state of the dianion could be assigned formally as Co(II), the noninnocent nature of the dithiolene ligand raised the possibility that protonation could take place at either the metal or sulfur.[47] A computational study of the catalyst with similar structure by Hammes-Schiffer[48] also suggested that following initial reduction of the catalyst to the dianion, two protonations occurred on different sulfur donors followed by a second reduction.

Fig. 5

Interestingly, when the metal center of the catalyst became Ni, the CV experiment was basically identical except that $Ni(BNT)_2^-/Ni(BNT)_2^{2-}$ appeared at -0.68 V vs. SCE. The complex with the more positive reduction potentials for ML_2^-/ML_2^{2-} was the more active catalyst.[24] This result precisely explained that $Ni(BNT)_2^-$ showed higher activity of H_2 evolution under the same conditions. However, Eisenberg and co-wokers found $Ni(BDT)_2^-$ complex exhibited poor catalytic behavior for the light-driven generation of H_2.[23] They thought the poor catalytic performance of $Ni(BDT)_2^-$ resulted from its highly cathodic electrocatalytic wave, which meant that the catalytic intermediate couldn't be reduced neither by PS^* nor PS^-. However, Roberts found that films electrodeposited onto glassy carbon electrodes from acidic acetonitrile solution of $Ni(BDT)_2^-$ were active toward electrocatalytic hydrogen production at potentials 0.2-0.4 V positive of untreated electrodes.[27] Generally speaking, the three-valence Ni(III) complexes are unstable. However, the nickel complexes with similar structures based on tdt ligand (tdt=toluene-3,4-dithiolate), for instance $Ni(tdt)_2^{2-}$, $Ni(tdt)_2^-$ and $Ni(tdt)_2$, had already been characterized in the literature, confirming three-valence nickel ion was unquestionably the most air stable of the three entries.[34]

Scheme 3

As stated above, the possible H_2 evolution mechanism of the metal dithiolene complexes in the photocatalytic system was illustrated in Scheme 3. Thus, $M(BNT)_2^-$ got an electron from excited $^{1*}EY^{2-}$ and $^{3*}EY^{2-}$ to form $M(BNT)_2^{2-}$, followed by rapidly protonated to give $H\text{-}M(BNT)_2^-$ intermediate. Subsequent reduction and reaction with H^+ lead to H_2 formation.

4. Conclusions

Two novel cobalt/nickel-dithiolene complexes for the photocatalytic hydrogen evolution in aqueous solutions had been synthesized and characterized. The H_2 evolution activity of **1/2** was estimated based on the constructed homogeneous photocatalytic system. The maximum H_2 yields of 495 TONs (vs. Cat.) for **1** and 676 TONs for **2** were recorded in 4 h irradiation under optimal conditions. The deactivation of photocatalytic system was mainly due to the photodegradation of EY^{2-}, and also slightly linked with that of the title complexes. In the photocatalytic process, the excited PS transported the electron to the WRC, following a multi-step reaction to produce H_2. Although the H_2 evolution activity was not high enough in this stage, the working principle had been illustrated, that is, the metal dithiolene complexes could be used as potential catalysts for conversion of solar energy to H_2 as a clean and renewable energy resource.

Acknowledgments

This work was supported by the National Natural Science Foundation of China (No. 21171147) and Henan Province Joint Funds of the National Natural Science Foundation of China (U1204522) and Program for Science & Technology Innovation Talents in Universities of Henan Province (13HASTIT033).

References

1 R. F. Service, Science 2005, **309**, 548-551.

2 H. B. Gray, Nat. Chem. 2009, **1**, 7.

3 N. S. Lewis and D. G. Nocera, Proc. Nat. Acad. Sci. U.S.A., 2006, **103**, 15729-15735.

4 K. Mazloomi and C. Gomes, Renewable Sustainable Energy Rev., 2012, **16**, 3024-3033.

5 P. Du, J. Schneider, P. Jarosz, J. Zhang, W. W. Brennessel and R. Eisenberg, J. Phys. Chem. B, 2007, **111**, 6887-6894.

6 E. D. Cline, S. E. Adamson and S. Bernhard, Inorg. Chem., 2008, **47**, 10378-10388.

7 P. N. Curtin, L. L. Tinker, C. M. Burgess, E. D. Cline and S. Bernhard, Inorg. Chem. 2009, **48**, 10498-10506.

8 D. N. Chirdon, W. J. Transue, H. N. Kagalwala, A. Kaur, A. B. Maurer, T. Pintauer and S. Bernhard, Inorg. Chem. 2014, **43**, 1487-1499.

9 C. Bachmann, M. Guttentag, B. Spingler and R. Alberto, Inorg. Chem., 2013, **52**, 6055-6061.

10 M. Nippe, R. S. Khnayzer, J. A. Panetier, D. Z. Zee, B. S. Olaiya, M. Head-Gordon, C. J. Chang, F. N. Castellano and J. R. Long, Chem. Sci., 2013, **4**, 3934-3945.

11 W. M. Singh, M. Mirmohades, R. T. Jane, T. A. White, L. Hammarström, A. Thapper, R. Lomoth and S. Ott, Chem. Commun., 2013, **49**, 8638-8640.

12 L. Tong, R. Zong and R. P. Thummel, J. Am. Chem. Soc., 2014, **136**, 4881-4884.

13 W. M. Singh, T. Baine, S. Kudo, S. Tian, X. A. N. Ma, H. Zhou, N. J. DeYonker, T. C. Pham, J. C. Bollinger, D. L. Baker, B. Yan, C. E. Webster and X. Zhao, Angew. Chem. Int. Ed., 2012, **51**, 5941-5944.

14 S. Varma, C. E. Castillo, T. Stoll, J. Fortage, A. G. Blackman, F. Molton, A. Deronzier and M. -N. Collomb, Phys. Chem. Chem. Phys., 2013, **15**, 17544-17552.

15 M. Natali, A. Luisa. E. Lengo and F. Scandola, Chem. Commun., 2014, **50**, 1842-1844.

16 V. Artero, M. Chavarot-Kerlidou and M. Fontecave, Angew. Chem., Int. Ed., 2011, **50**, 7238-7266.

17 Y. Lin, G. Yuan, S. Sheehan, S. Zhou and D. Wang, Energy Environ. Sci., 2011, **4**, 4862-4869.

18 P. Du and R. Eisenberg, Energy Environ. Sci., 2012, **5**, 6012-6021.

19 M. R. Dubois and D. L. Dubois, Acc. Chem. Res., 2009, **42**, 1974-1982.

20 U. J. Kilgore, J. A. S. Roberts, D. H. Pool, A. M. Appel, M. P. Stewart, M. R. DuBois, W. G. Dougherty, W. S. Kassel, R. M. Bullock and D. L. DuBois, J. Am. Chem. Soc., 2011, **133**, 5861-5872.

21 M. L. Helm, M. P. Stewart, R. M. Bullock, M. R. DuBois and D. L. DuBois, Science, 2011, **333**, 863-866.

22 M. P. McLaughlin, T. M. McCormick, R. Eisenberg and P. L. Holland, Chem. Commun., 2011, **47**, 7989-7991.

23 W. R. McNamara, Z. Han, P. J. Alperin, W. W. Brennessel, P. L. Holland and R. Eisenberg, J. Am. Chem. Soc., 2011, **133**, 15368–15371.

24 W. R. McNamara, Z. Han, C. J. (Madeline) Yin, W. W. Brennessel, P. L. Holland and R. Eisenberg., Proc. Nat. Acad. Sci. USA., 2012, **109**, 15594-15599.

25 Z. Han, W. R. McNamara, M. S. Eum, P. L. Holland and R. Eisenberg, Angew. Chem., Int. Ed., 2012, **51**, 1667-1670.

26 H. N. Kagalwala, E. Gottlieb, G. Li, T. Li, R. Jin and S. Bernhard, Inorg. Chem., 2013, **52**, 9094-9101.

27 M. Fang, M. H. Engelhard, Z. Zhu, M. L. Helm and J. A. S. Roberts, ACS Catal., 2014, **4**, 90-98.

28 S.-P. Luo, E. Meja, A. Friedrich, A. Pazidis, H. Junge, A. E. Surkus, R. Jackstell, S. Denurra, S. Gladiali, S. Lochbrunner and M. Beller, Angew. Chem., Int. Ed., 2013, 52, 419 –423.

29 T. Lazarides, T. McCormick, P. Du, G. Luo, B. Lindley and R. Eisenberg, J. Am.Chem. Soc., 2009, **131**, 9192-9194.

30 Z. Y. Wang, H. Rao, M.-F. Deng, Y. T. Fan and H. W. Hou, Phys. Chem. Chem. Phys., 2013,**15**, 16665-16671.

31 A. W. -H. Mau, O. Johansen and W. H. F. Sasse, Photochem. Photobiol., 1985, **41**, 503-509.

32 C. Baffert , V.t Artero and M. Fontecave, Inorg. Chem., 2007, **46**, 1817-1824.

33 M. E. Carroll, B. E. Barton, D. L. Gray, A. E. Mack and T. B. Rauchfuss, Inorg. Chem., 2011, **50**, 9554-9563.

34 M. J. Baker-Hawkes, E. Billig and H. B. Gray, J. Am. Chem. Soc., 1966, **88**, 4870-4875.

35 D. D. Perrin and W. L. F. Armarego, Purification of Laboratory Chemicals, 3rd ed., Pergamon Press, New York, 1988.

36 H. He, L.-Y. Chen, W.-Y. Wong, W.-H. Chan and A. W. M. Lee, Eur. J. Org. Chem., 2010, **22**, 4181-4184.

37 P. Machata, P. Herich, K. Lušpai, L. Bucinsky, S. Šoralová, M. Breza, J. Kozisek, and P. Rapta, Organometallics, 2014, **33**, 4846-4859.

38 C. V. Krishnan and N. Sutin, J. Am. Chem. Soc., 1981, **103**, 2141-2142.

39 Q. Li and G. Lu, J. Mol. Catal. A: Chem., 2007, **266**, 75-79.

40 P. Du, K. Knowles and R. Eisenberg, J. Am. Chem. Soc., 2008, **130**, 12576-12577.

41 N. O. McHedlov-Petrossyan, V. I. Kukhtik and V. D. Bezugliy, J. Phys. Org. Chem., 2003, **16**, 380-397.

42 T. Shimidzu, T. Iyoda and Y. Koide, J. Am. Chem. Soc., 1985,**107**, 35-41.

43 J. Dong, M. Wang, P. Zhang, S. Yang, J. Liu, X. Li and L. Sun, J. Phys. Chem. C, 2011, **115**, 15089–15096.

44 S. D. M. Islam, T. Konishi, M. Fujitsuka, O. Ito, Y. Nakamura and Y. Usui, Photochem. Photobiol., 2000, **71**, 675-680.

45 J. P. Bigi, T. E. Hanna, W.H. Harman, A. Chang and C. J. Chang, Chem. Commun., 2010, **46**, 958-960.

46 H. I. Karunadasa, C. J. Chang and J. R. Long, Nature, 2010, **464**, 1329-1333.

47 S. Sproules and K. Wieghardt, Coord. Chem. Rev., 2011, **255**, 837-860.

48 B. H. Solis and S. Hammes-Shiffer, J. Am. Chem. Soc., 2012, **134**, 15253-15256.

Figure captions

Scheme 1 A schematic illustration of photocatalytic H_2 evolution from cobalt/nickel dithiolene complex.

Scheme 2 Synthetic route of **1**.

Sheme 3 Possible H_2 evolution mechanism of the cobalt /nickel dithiolene complex in the photocatalytic system.

Fig.1 Effect of solvent on hydrogen generation at the fixed conditions with **1** (0.1 mM), EY^{2-} (0.4 mM) and TEA (10%) in the mixture of organic solvent and water in 4.0 h irradiation (λ>420 nm).

Fig.2 Effect of medium pH value on hydrogen generation with catalyst (**1**/**2**, 0.1 mM), EY^{2-} (0.4 mM) and 10% TEA in CH_3CN/H_2O (1:1, v/v) over 4 h irradiation (λ>420 nm)

Fig.3 (a) Changes of H_2 evolution with irradiation time before and after adding EY^{2-} (8 μmol) or **1** (2 μmol) in the photocatalytic system containing EY^{2-} of 0.4 mM, **1** of 0.1mM, 10% TEA and pH 10.0 in CH_3CN/H_2O (1:1, v/v) after 4 h of irradiation(λ>420 nm). (b) Change of absorption spectra with irradiation time in a 1 cm quartz cell for photocatalytic system containing **1** (0.1 mM), EY^{2-} (0.4 mM), 10%TEA (v/v) and pH 10.0 in CH_3CN/H_2O (1/1, v/v).

Fig. 4 (a) Fluorescence spectra of EY^{2-} (1.0×10^{-5} M) in CH_3CN/H_2O (1:1, v/v) with concentration of **1** ranging from 0 to 70 equiv; Inset: the corresponding Stern-Volmer polt of $[I_0/I]$ *verse* concentration of quencher. (b) Fluorescence spectra of EY^{2-} (1.0×10^{-5} M) in CH_3CN/H_2O (1:1, v/v) with concentration of **2** ranging from 0 to 30 equiv; Inset: the corresponding Stern-Volmer polt of $[I_0/I]$ *verse* concentration of quencher.

Fig. 5 (a) Cyclic voltammograms of 1.0 mM **1** in a 0.1 M solution of KNO_3 in 1:1 CH_3CN/H_2O with concentration of TFA ranging from 2.0 mM to 8.0 mM. Scan Rate: 100 mV/s with a glassy carbon working electrode, Pt auxiliary electrode, and SCE reference electrode. (b) Cyclic voltammograms of 1.0 mM **2** under the same conditions.

Table1 Effect of molar ratio of PS/ WRC (**1**) on hydrogen generation*

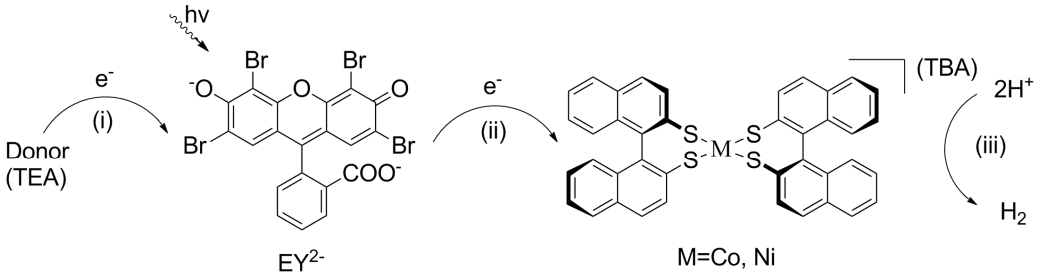

(i) Reductive quenching (ii) Intermolecular ET (iii) Catalytic proton reduction

Scheme 1

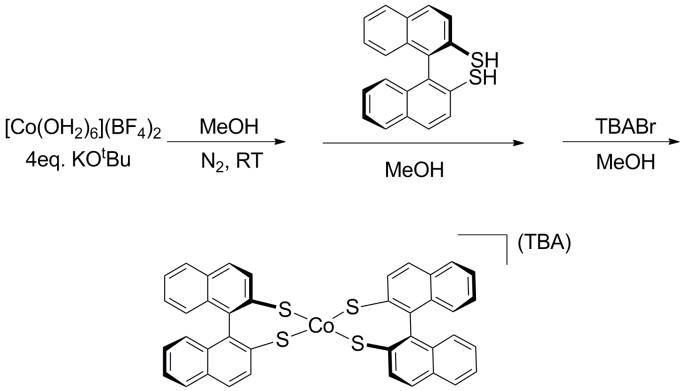

Scheme 2

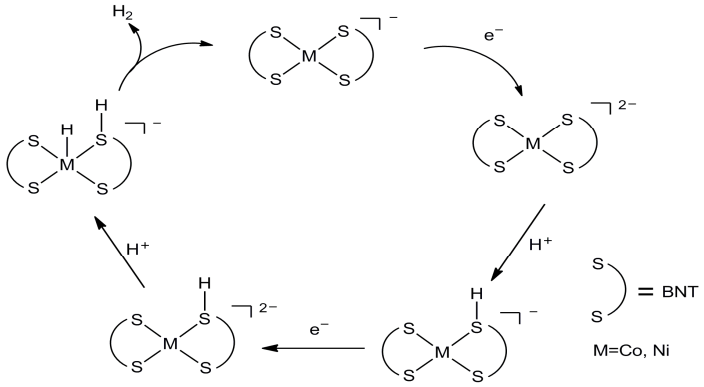

Scheme 3

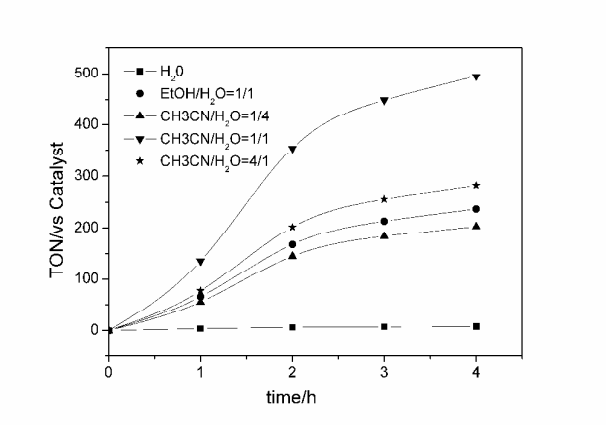

Fig. 1

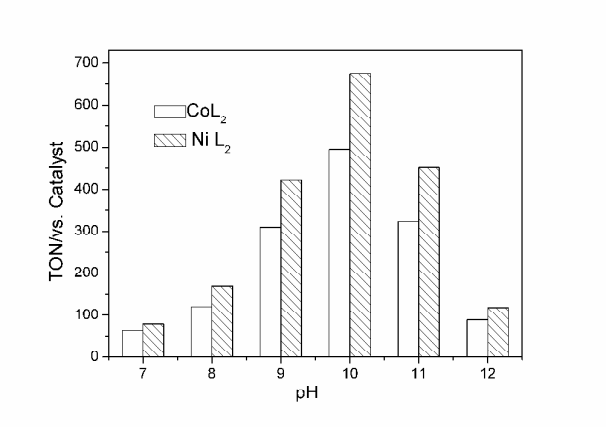

Fig. 2

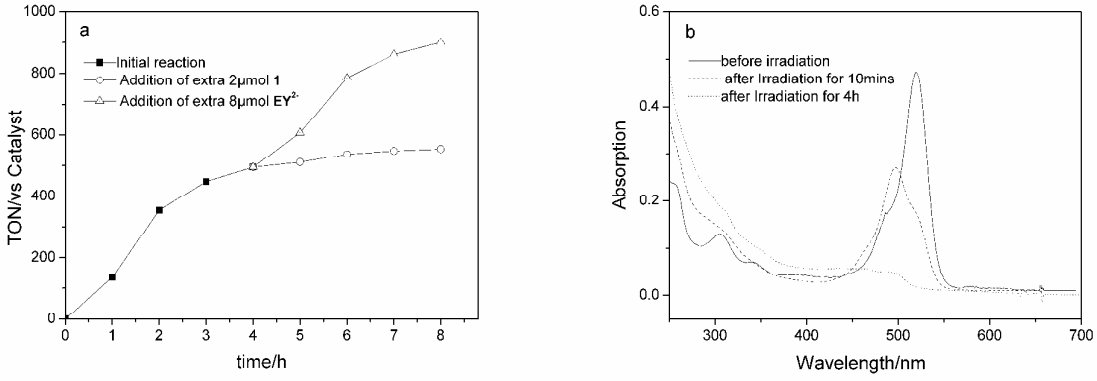

Fig. 3

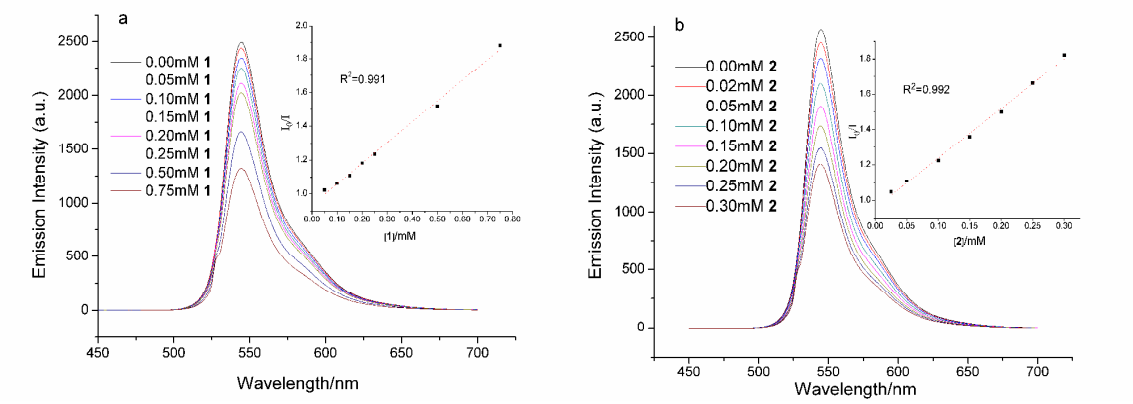

Fig. 4

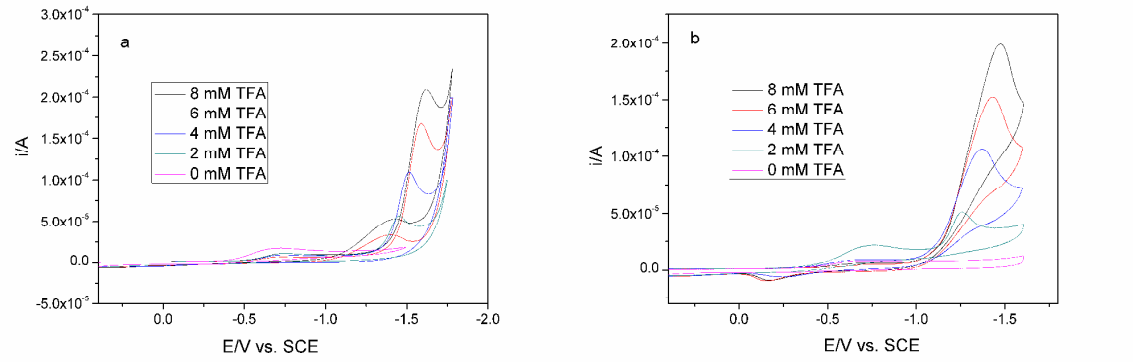

Fig. 5

Serial No	PS Conc. (mM)	WRC Conc. (mM)	PS/WRC (mol/mol)	TONs (vs. WRC)
1	0.4	0.1	1:0.25	495
2	0.4	0.2	1:0.5	326
3	0.4	0.4	1:1	152
4	0.8	0.4	2:1	197
5	1.6	0.4	4:1	237

*Reaction conditions: **1** as WRC, EY^{2-} as PS and TEA (10%) in 1:1 CH_3CN/H_2O under N_2 atmosphere at pH=10 (λ>420nm).

Table 1